Phase Structure and Property Relationships in Ternary Polypropylene/Elastomer/Filler Composites: Effect of Elastomer Polarity

K. PREMPHET, P. HORANONT

Department of Chemistry, Mahidol University, Rama VI Road, Bangkok 10400, Thailand

ABSTRACT: Ternary composites of polypropylene (PP), elastomer, and calcium carbonate (CaCO$_3$) filler were prepared to study their structure/property relationships. Two kinds of phase structure were formed, depending on the elastomer present in the composites. Separation of elastomer and filler particles was found when a nonpolar ethylene–octene copolymer was used. Encapsulation of filler by the elastomer was achieved by using a polar ethylene–vinyl acetate elastomer. The mechanical properties of ternary composites were strongly dependent on material composition and their phase structures. In the present study, composites with separate dispersion structure showed higher modulus and impact strength than those of encapsulation type. The deformation mechanisms of both composites were studied using scanning electron microscopy. © 2000 John Wiley & Sons, Inc. J Appl Polym Sci 76: 1929–1939, 2000

Key words: polypropylene; ternary composite; phase structure; mechanical properties

INTRODUCTION

Ternary phase composites consisting of a polymer matrix, elastomer inclusion, and particulate filler have become attractive materials for numerous engineering applications. The mechanical properties of such composites are determined not only by composition, but also by the phase morphology present, in particular the relative dispersion of additive components. Two cases of composite morphology may be found,[1–14] either elastomer and filler particles dispersed separately in the polymer matrix or elastomer encapsulated filler particles forming core–shell inclusion structure. Pukanszky et al.[4–5] investigated the ternary composites of polypropylene (PP), ethylene–propylene diene terpolymer (EPDM), and calcium carbonate (CaCO$_3$) and found that the surface treatment of the filler being the most important parameter controlling the composite phase structure. Untreated CaCO$_3$ filler was found to be extensively encapsulated by the incorporated elastomer, whereas elastomer de-encapsulated from filler surface when the stearic acid coated CaCO$_3$ was used. Our earlier studies on the structure and properties of PP composites containing ethylene–octene copolymer (EOR) and CaCO$_3$ has shown contradictory results.[17] Stearic acid treatment of filler particles showed no effect either on the dispersion or the interaction of filler and polymer components.

Various methods have been applied in order to control these phase structures. In PP/EPR/CaCO$_3$ composites, a complete separation was extensively promoted by adding functionalized PP to the composite, whereas a complete encapsulation was achieved by using functionalized elastomer.[3,6]

These distinct morphologies gave significantly different tensile and impact properties. Ternary composites with a separation structure have been reported to have higher modulus and tensile yield stress than those containing encapsulated filler,[6–9] whereas composites with an encapsulation structure exhibited a higher impact strength.[2,6,9] However, the contrasting result was reported by Kolarik and Jancar[3] for PP/EPR/CaCO$_3$ composite, in which composites containing encapsulated particles have lower impact strength than composites with a separation structure.

The objective of the present study was to investigate the effects of type and composition of elastomer on the phase microstructure and mechanical properties of PP/elastomer/filler composites. Two elastomers examined were EOR and ethylene–vinyl acetate (EVA) elastomer, which are representative of nonpolar and polar elastomers, respectively. CaCO$_3$ without any surface treatment was used as a standard filler.

EXPERIMENTAL

Materials

Polypropylene (PP) homopolymer P400S [melt flow rate (MFR) = 4.1 g/10 min] supplied by Thai Polyethylene Co. was used as the matrix polymer. Two elastomers used were EOR Engage 8150, consisting of 25 wt % octene with a MFR of 0.5 g/10 min, and EVA Elvax 460, having 18 wt % vinyl acetate and a MFR of 2.4 g/10 min. Both were supplied by Dupont Dow Elastomer Co. The filler used was calcium carbonate (CaCO$_3$) grade Microcal from Lime Quality Co.(Thailand), with an average particle diameter of 5.3 μm and specific surface area of 1.8 m^2/g.

Compounding

In this study, the PP masterbatch containing 35 vol % CaCO$_3$ filler was prepared in a corotating twin screw extruder (Prism TSE 16). The masterbatch was then melt-mixed with elastomer in various ratios to achieve the required concentration of elastomer and filler in the PP matrix. The melt blending was performed at 160–190°C (from feed zone to die), with a screw speed of 220 rpm.

Characterization of Structure and Properties

Phase microstructures of the composites were examined by scanning electron microscopy (SEM).

Specimens were prepared by immersing impact test pieces in liquid nitrogen, before fracturing them using an impact-testing machine. The fractured surfaces were then exposed to hot heptane vapor for 20 s in order to remove the elastomer particles from the composites, thus improving contrast between the PP matrix and elastomer phases. The surfaces prepared were platinum/palladium sputter-coated and examined in a Hitachi S2500 scanning electron microscope (Tokyo, Japan).

The melting and crystallization behavior of the composites was studied using a Perkin-Elmer DSC-7 differential scanning calorimeter (DSC; Norwalk, CT). Samples were first heated from 50 to 230°C at a scan rate of 10°C/min and then maintained at 230°C for 5 min before cooling to 50°C at the same rate. Melting and crystallization thermograms were recorded.

Tensile properties were measured in accordance with ASTM D638-89, using a tensile testing machine (Model 4301; Instron, Canton, MA) with a crosshead speed of 50 mm/min. Izod impact strength was obtained from notched specimens, using a pneumatic impact tester (Radmana ITR-2000). An impact velocity of 3.4 m/s was used. After each test, a force–displacement curve was obtained. The value of impact strength in terms of initiation, propagation, and failure energy were calculated. All mechanical testing was undertaken at 23°C.

RESULTS AND DISCUSSION

Phase Structure Analysis

SEM micrographs of the etched cryogenic fracture surfaces of PP/EOR/CaCO$_3$ and PP/EVA/CaCO$_3$ composites are shown in Figure 1. The dark holes represent the elastomer droplets, which are dissolved out by selective etching, whereas brighter irregular shape particles are of CaCO$_3$ filler. A SEM micrograph [Fig. 1(a)] reveals a separate dispersion of EOR and CaCO$_3$ particles in the PP matrix. The size of EOR dispersed particles was approximately 0.2 μm.

A contrasting morphology is shown in Figure 1(b) for the PP/EVA/CaCO$_3$ composite, where EVA encapsulated the filler particles, forming a core–shell inclusion structure. After etching, voids were observed around the filler particles. Apart from forming an interlayer around the filler particles, EVA also appeared as small dispersed
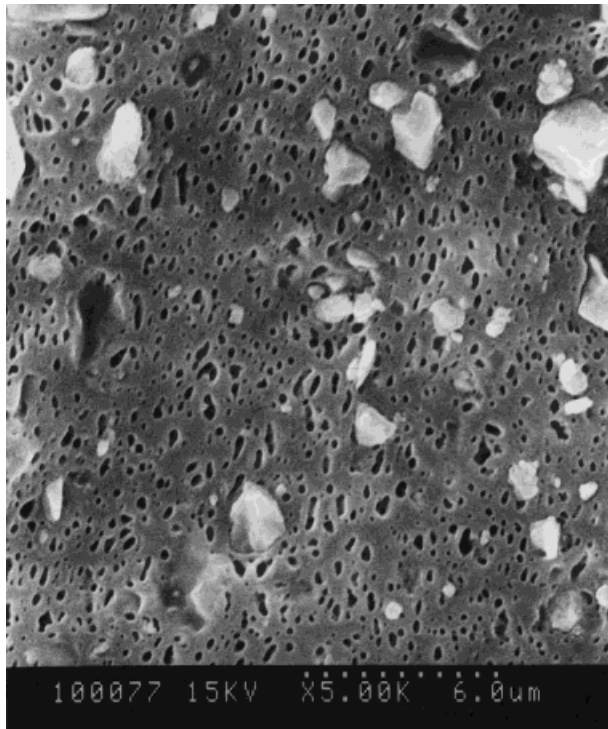
(a)
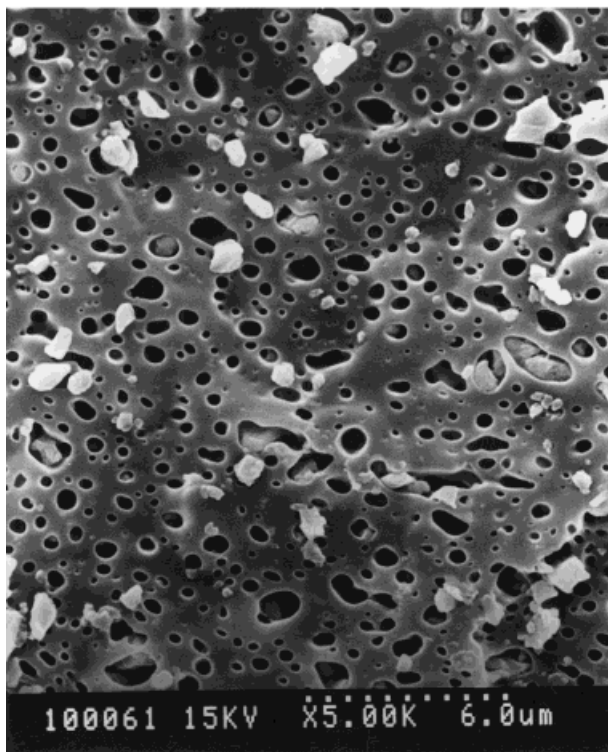
(b)

Figure 1 Cryogenic fractured and etched surfaces of ternary phase PP composites. (a) PP/EOR/CaCO$_3$ (60/30/10); (b) PP/EVA/CaCO$_3$ (60/30/10).

droplets in the PP matrix. A previous study on phase structure formation of these composites revealed that the main factor determining the composite phase structure was the surface characteristics of the components, e.g., wetability, surface energy, and interfacial adhesion between phases, whereas the composite formulation and mixing sequences of each component produced only a minor effect.[15]

Apart from SEM observations, the location of the elastomer in the ternary composites was successfully determined by the use of DSC technique. Table I shows the T_c, $T_{c\ onset}$, and T_m of various PP composites. In the binary system, the incorporation of 40% elastomer (either EOR or EVA) without filler slightly changed the T_c, $T_{c\ onset}$, and T_m of PP. In contrast, the T_c and $T_{c\ onset}$ of PP increased significantly when 40% CaCO$_3$ was incorporated. This indicated that the presence of CaCO$_3$ markedly influenced the crystallization behavior of PP by acting as a nucleating agent, promoting the crystallization of PP. By considering changes in the T_c and $T_{c\ onset}$ values of the composites, the effect of elastomer and filler on the crystallization of PP in various ternary composites could be evaluated, and as a consequence, the phase structure could be verified.

In the PP/EOR/CaCO$_3$ composites, a strong nucleating effect of CaCO$_3$ was clearly observed. The T_c and $T_{c\ onset}$ values were found to increase considerably as the CaCO$_3$ content increased. This result implied a direct contact of CaCO$_3$ to PP or a separate dispersion structure in this system. Contrary results were found for PP/EVA/CaCO$_3$ composites, in which no influence of CaCO$_3$ on the T_c and $T_{c\ onset}$ values was observed. Both values were constant up to 30 vol % filler. The reduction in nucleating efficiency of the filler in the PP/EVA/CaCO$_3$ system was, therefore, a result of the encapsulation of filler particles by EVA.

Tensile Properties

The influence of EOR, EVA, and CaCO$_3$ on composite tensile properties is shown in Table II. Incorporation of elastomers to PP caused a reduction in tensile stress of both binary PP/EOR and PP/EVA blends. The reduction in tensile stress became more pronounced when CaCO$_3$ was incorporated into the PP/EOR blends. The contrary results were observed for the PP/EVA/CaCO$_3$ composites. As the volume fraction of filler increased, the yield stress increased. The increase in tensile yield stress after filler loadings may be

Table I   Crystallization (T_c), the Onset of Crystallization ($T_{c\ onset}$), and Melting Temperatures (T_m) of Various Ternary Phase PP Composites

PP/Elastomer/CaCO₃ (vol %)	T_c (°C)		$T_{c\ onset}$ (°C)		T_m (°C)	
	EOR	EVA	EOR	EVA	EOR	EVA
100/0/0	111.0		115.1		162.1	
60/40/0	109.6	110.0	113.9	113.3	164.9	162.3
60/35/5	114.8	110.0	119.2	113.5	164.3	164.4
60/30/10	122.8	110.0	130.1	113.4	163.3	161.9
60/20/20	130.5	110.0	135.6	113.4	163.6	162.0
60/10/30	132.5	109.5	137.2	113.6	163.6	162.3
60/0/40	133.0		137.3		165.8	

attributed to the improved adhesion between the CaCO₃ filler and polar EVA phase, brought about by acid–base interaction, owing to the interfacial forces of vinyl acetate toward the CaCO₃ surfaces. Similar behaviors have been found in CaCO₃ filled poly(vinyl acetate) composites.[16]

Comparing the tensile modulus of ternary composites of PP/EOR/CaCO₃ and PP/EVA/CaCO₃ is shown in Table II and Figure 2. It is evident that incorporation of 40% elastomer markedly reduced the modulus of PP, whereas the addition of filler noticeably increased the modulus of the ternary PP/EOR/CaCO₃ composites. The differences in composite modulus by the use of EOR and EVA were very small at the filler content less than 10%, but they became more pronounced with increasing filler content. At filler contents higher than 10%, all ternary composites containing EVA showed lower modulus values than those with EOR. To investigate the effect of phase structure on composite modulus, Nielsen's model (eq. 1)[18] for calculating modulus of filled polymer was applied.

$$E_R = \frac{E_c}{E_m} = \frac{1 + AB\nu_f}{1 - B\psi\nu_f} \tag{1}$$

where

$$B = \frac{(E_f/E_m) - 1}{(E_f/E_m) + A} \quad \text{and} \quad \psi = 1 + \left(\frac{1 - \phi_m}{\phi_m^2}\right)\nu_f.$$

E_R is the relative modulus, E_c is the modulus of the composite, E_m is the modulus of the matrix polymer, E_f is the modulus of the filler, ν_f is the volume fraction of filler, and ϕ_m is maximum volume fraction of filler. Experimental modulus data of the corresponding two phase of PP/elastomer blends were taken as the matrix value for the ternary phase systems, assuming that the elastomer and filler particles act independently in the PP matrix.

The results of Figure 2 shows that the modulus data of PP/EOR/CaCO₃ composites fit reasonably well with the data calculated from Nielsen's equation at every additive content. This proved that

Table II   Tensile Properties of Ternary Phase PP Composites

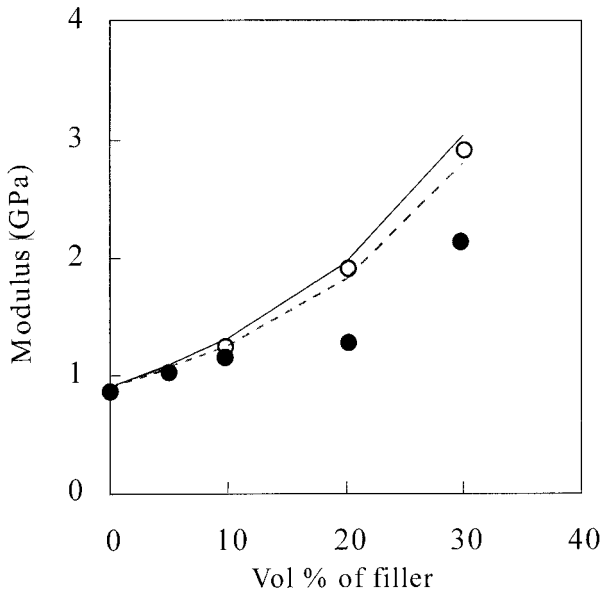| PP/Elastomer/CaCO₃ (vol %)	Yield Stress (MPa)		Modulus (GPa)		Elongation at Break (%)	
	EOR	EVA	EOR	EVA	EOR	EVA
100/0/0	34.4		1.6		>350	
60/40/0	18.8	20.1	0.9	0.9	>350	335.9
60/35/5	18.0	21.0	1.0	1.0	>350	340.7
60/30/10	17.6	21.4	1.2	1.1	309.7	327.6
60/20/20	17.1	23.1	1.9	1.3	248.3	21.2
60/10/30	17.1	24.2	2.9	2.3	20.4	7.2

Figure 2 Tensile modulus of ternary phase PP composites. Dashed lines and solid lines are of PP/EOR/$CaCO_3$ and PP/EVA/$CaCO_3$, respectively, using Nielsen's equation. ○, composites containing EOR; ●, composites containing EVA.

the composite structure does not change with composition and that the components are always separately dispersed in the PP matrix. In contrast, a deviation from theoretical calculation was observed in the PP/EVA/$CaCO_3$ composites in which the measured modulus of PP/EVA/$CaCO_3$ composites were lower than the predictive ones. This indicated that the reinforcing efficiency of filler in the PP/EVA/$CaCO_3$ composites was suppressed by the surrounding EVA layer because of their encapsulation structure. The lowering in modulus of the composites with an encapsulation structure was reportedly due to the volume of low modulus elastomer inclusion extended by the

rigid filler core, thus leading to a decrease in composite modulus.[9]

Impact Properties

Table III shows the notched Izod impact energies of various PP composites. PP failed in a brittle manner with a low crack initiation and propagation energies. In binary blends, impact resistance of PP was significantly increased by the incorporation of elastomers, in particular EOR. The impact failure energy of a PP/EOR blend was found to be 24 times higher than that of pure PP. Comparing the effects of EOR and EVA on the failure energy of ternary composites, it can be seen that EOR again was far more effective in raising composite impact resistance relative to PP. In the case of PP/EVA/$CaCO_3$ composites, the overall impact energy was governed more by the crack initiation energy, reflecting a good adhesion between an elastomer layer and filler particles in the system. Because in the PP/EOR/$CaCO_3$ composites the energy required for the crack propagation process was high, it was therefore the main energy for impact improvement in the composites.

Adams and Wu[19] and Merle et al.[20] studied nylon–rubber blends with instrumented impact testing. From load–time curves they deduced that energy absorption in brittle fracture only took place at crack initiation, whereas in tough fracture large energy absorption also occurred during crack propagation. Our results agreed well with their findings.

The differing in impact resistance of both composite systems may be caused partly by the properties of elastomer itself. To eliminate the effect of elastomer characteristics, the relative impact strength was considered. Plots of the relative impact failure energy as a function of filler concen-

Table III   Impact Properties of Ternary Phase PP Composites

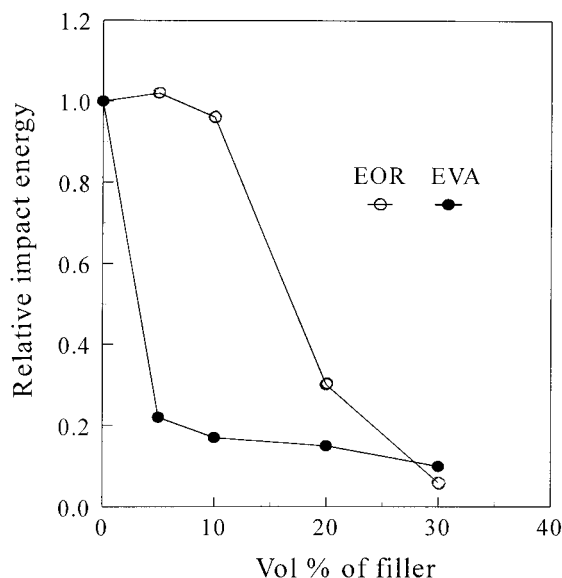| PP/Elastomer/$CaCO_3$ (vol %)	Initiation Energy (J/m)		Propagation Energy (J/m)		Failure Energy (J/m)	
	EOR	EVA	EOR	EVA	EOR	EVA
100/0/0	15.7		16.4		32.1	
60/40/0	201.1	98.9	574.9	180.6	777.2	279.5
60/35/5	173.5	40.6	622.5	22.5	796.0	62.6
60/30/10	153.3	32.4	596.5	17.7	749.8	50.1
60/20/20	82.3	24.5	153.1	16.0	235.4	40.5
60/10/30	24.8	15.5	24.5	13.8	49.2	29.3

Figure 3 Effect of filler content on the relative impact energy of PP composites. ○, composites containing EOR; ●, composites containing EVA.

tration are presented in Figure 3. In the case of PP/EOR/CaCO$_3$ composites, the relative impact energy was constant up to 10% filler loadings, a sudden drop in impact energy occurred at the filler content between 10% and 20%. A sharp decrease of the impact energy was accompanied by changes in the fracture mode from tough to brittle. Further increase of filler concentration beyond 20% caused only a slight drop in the impact energy. In the PP/EVA/CaCO$_3$ composites, although an encapsulation of filler by elastomer was achieved, a drop in composite impact strength due to the filler addition could not be prevented. The impact energy decreased suddenly as the filler was incorporated. The differences between the properties of these two types of composites were very small at high concentration of filler (30%) or low concentration of elastomer (10%), but they became more pronounced with rising elastomer content. This means that small concentration of elastomers do not have any beneficial influence on impact properties, regardless of whether they are dispersed separately or elastomer encapsulates the filler particle. At higher elastomer volume fractions (>10%), the results of this study showed that separately dispersed phases of elastomer and filler were apparently more effective impact modifiers than encapsulated structures of the same composition.

Observations on Impact Fracture Surface Morphology

Figure 4(a) shows a SEM micrograph of a fracture surface of a tested PP sample. It is evident that PP exhibited predominantly brittle fracture. Incorporation of EOR to PP caused extensive plastic deformation on the fracture surface [Fig. 4(b,c)]. This, however, was not observed for the PP/EVA system [Fig. 5(a,b)]. The fracture surface showed much less plastic deformation than the samples of PP/EOR blend. The semibrittle failure observed in the PP/EVA blend was partly due to a poor adhesion between EVA droplets and the PP matrix. The SEM of Figure 5(b) reveals a debonding of EVA particles from the PP matrix, due to a poor adhesion between the phases. Figure 6 is a general view of an impact fractured surface from a PP/elastomer/filler specimen showing three distinct areas. Area A is the fractured inductive area next to the notch, area B is the area in the middle of the fracture surface, and area C is located further away from the notch. The location of the features shown in Figures 7 and 8 for the ternary phase of PP/EOR/CaCO$_3$ and PP/EVA/CaCO$_3$ composites is labeled as A–C in Figure 6.

In the PP/EOR/CaCO$_3$ composites, stress whitening took place over the whole fracture surface and progressively increased in size as the EOR concentration increased. The fracture surface of Figure 7 reveals plastic deformation of the PP matrix and extensive cavitation, resulting from debonding of the filler particles. These cavities are evidently the source of the whitening observed in this sample. In the range of EOR concentration, regular striations associated with heavy plastic deformed fibril of the PP matrix were seen perpendicular to the direction of crack propagation [Fig. 7(c)]. Such striations also were found in the binary PP/EOR blends[15] and have been reported earlier in other rubber modified polymers.[21,22] Figure 8 demonstrates the characteristics of the fracture in PP/EVA/CaCO$_3$ (60/30/10) composites. This composite exhibited an encapsulation structure with impact energy only slightly higher than that of pure PP and much lower than that of PP/EOR/CaCO$_3$ composite of the same volume composition. Comparing the PP/EOR/CaCO$_3$ composites, the fracture surface of PP/EVA/CaCO$_3$ composites was rather flat and showed stress whitening only in the area near the notch tip (area A). Its fracture contained much less plastic deformation and no striation perpendicular to the direction of crack propagation. The
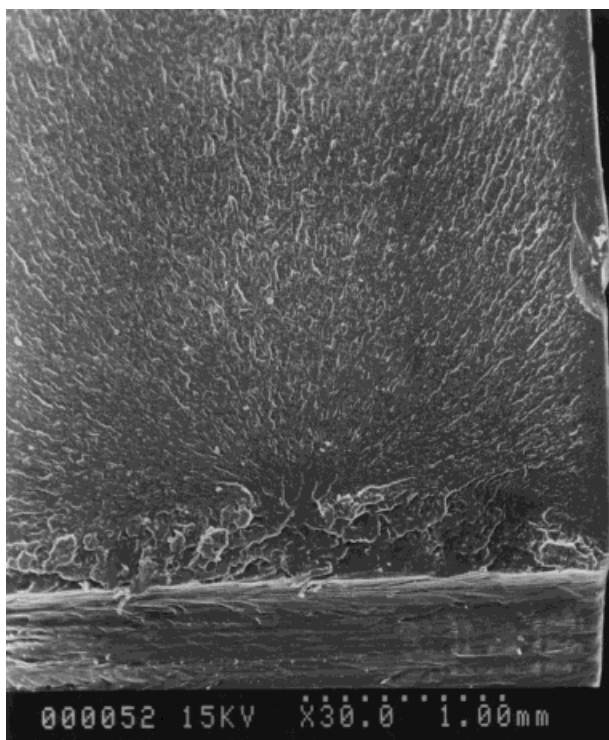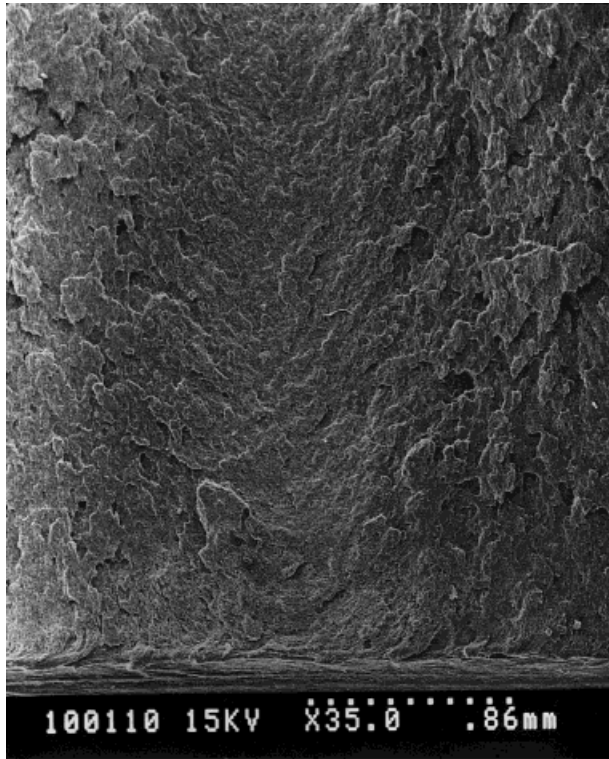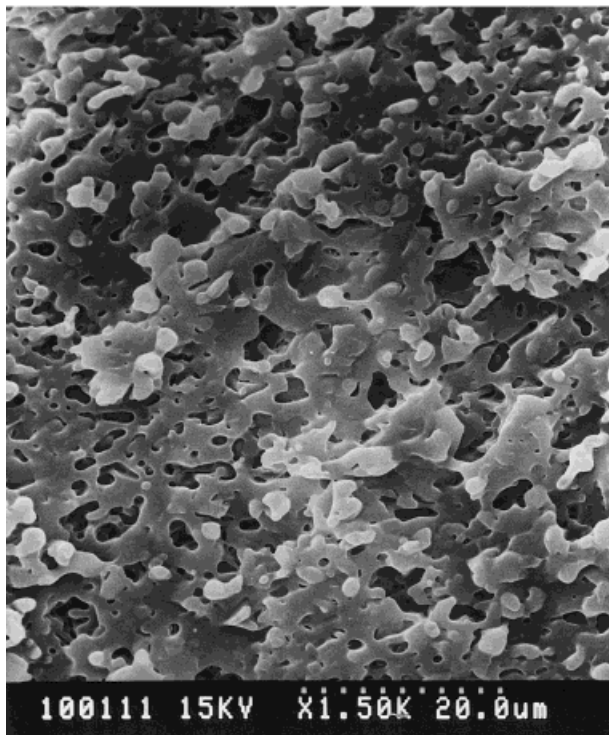
(a)

(b)
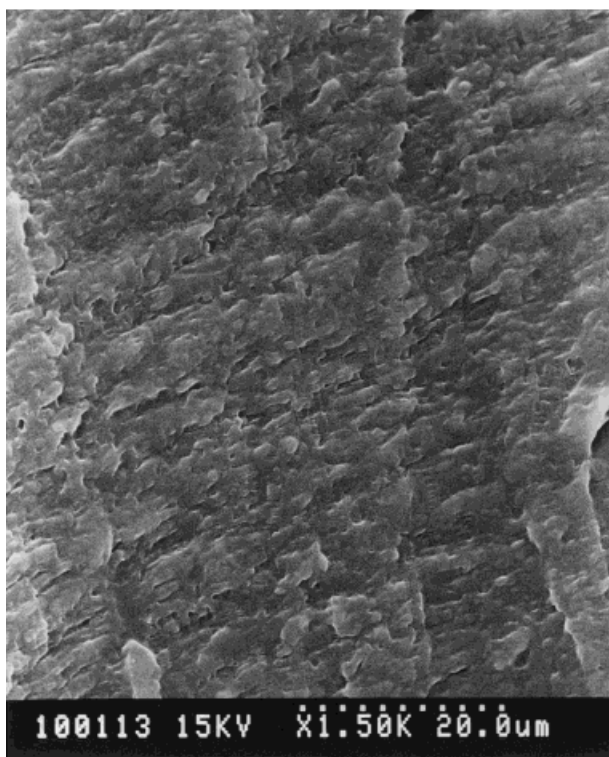
(c)

Figure 4 Impact fractured surfaces of PP and PP/EOR blends. (a) Pure PP; (b) PP/EOR (60/40) at low magnification; (c) high magnification of (b).

(a)

(b)

Figure 5 Impact fractured surfaces of PP/EVA blends. (a) PP/EVA (60/40) at low magnification; (b) high magnification of (a).
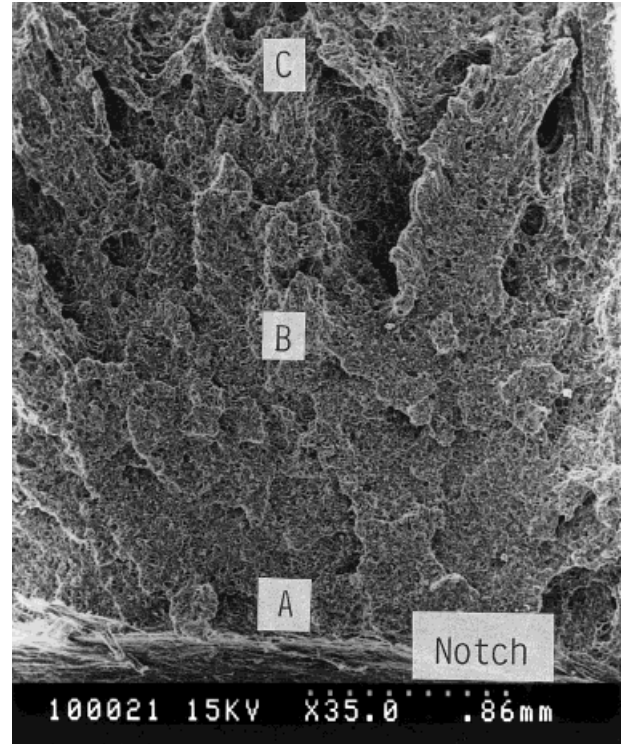

Figure 6 A general view of impact fractured surfaces of ternary phase PP composites. Area (A) is the fracture inductive area next to the notch; area (B) is the area in the middle of the fractured surface; area (C) is the area located further away from the notch.

poor impact performance of composites with encapsulation structure could be due to several reasons. Kolarik and Jancar[3] proposed several likely causes, including the improper core–shell particle size and shell modulus, which were less effective for interconnection of local microzones of the yielded matrix. In this study, another possible reason is believed to be due to a reduced affinity of the polar EVA to the PP matrix, therefore, leading to a decrease in the interfacial adhesion of the PP matrix both to the core–shell inclusions and to the dispersed EVA droplets. Thus, cracks propagated along those interfaces during the impact fracture, result in a poor impact strength in the composites.
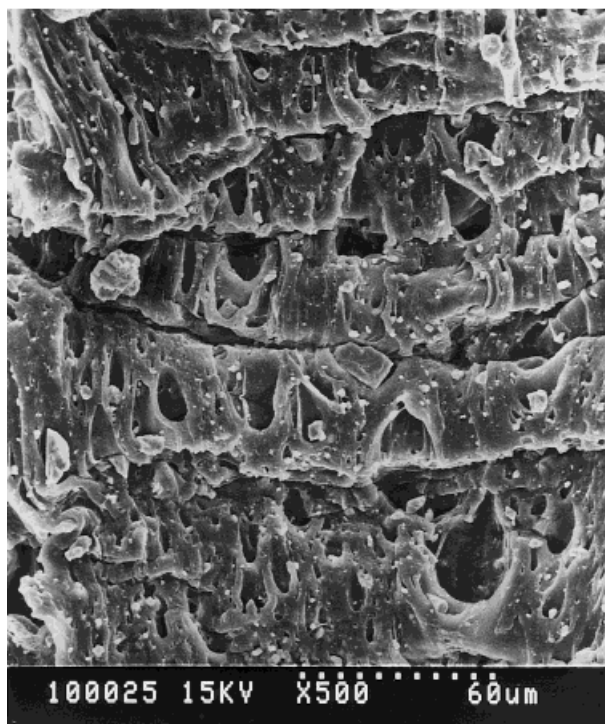
CONCLUSIONS

The effects of type and composition of elastomer on phase structure and mechanical properties of ternary PP composites containing elastomer and $CaCO_3$ filler were investigated. Phase structure
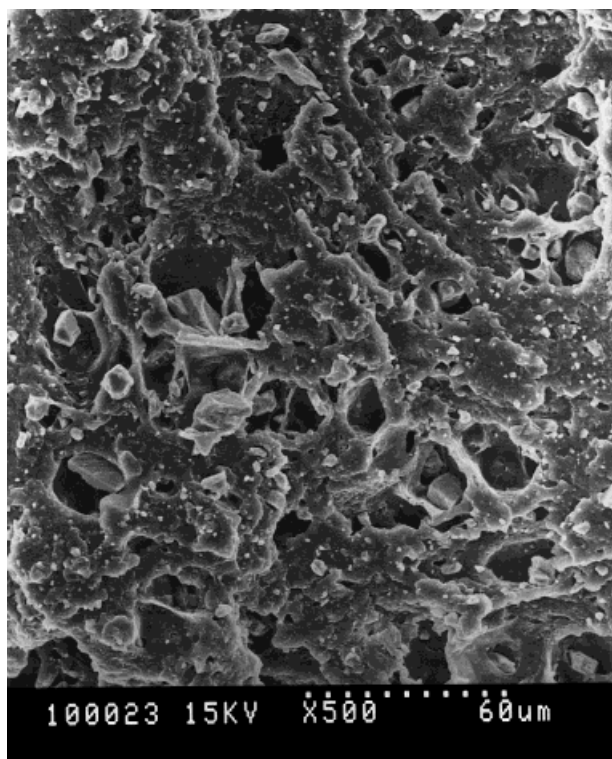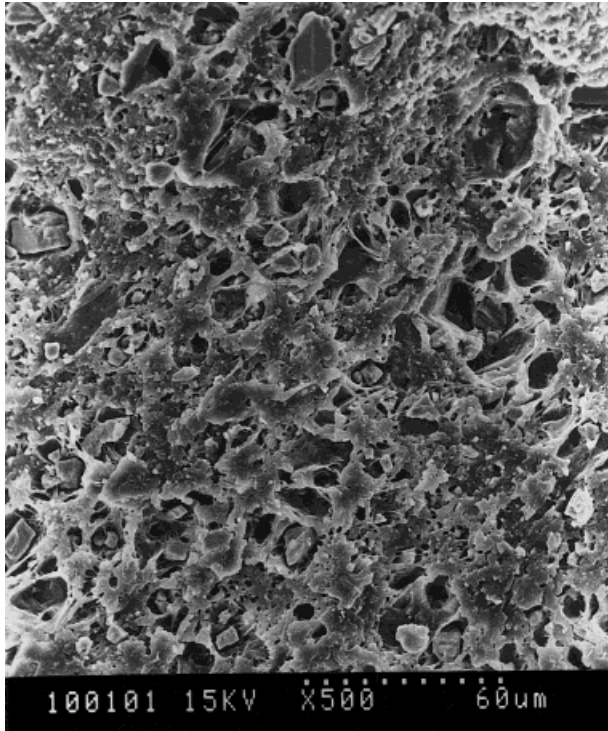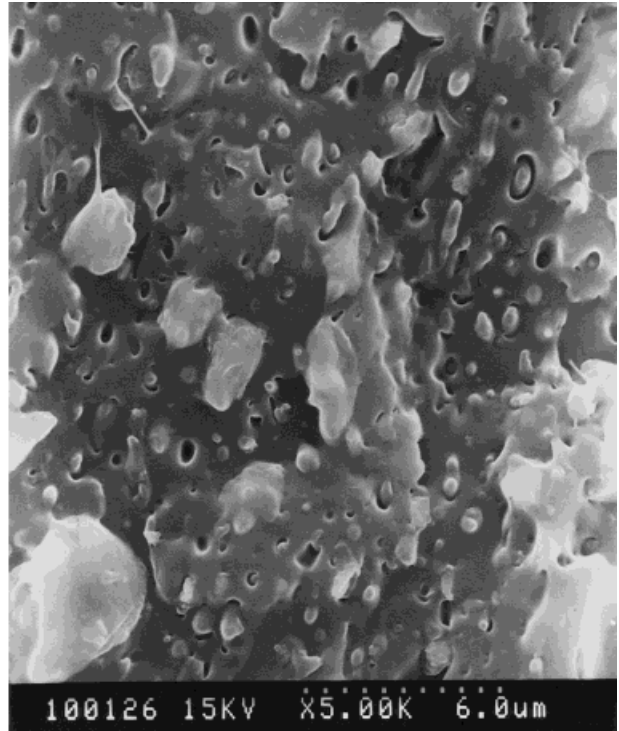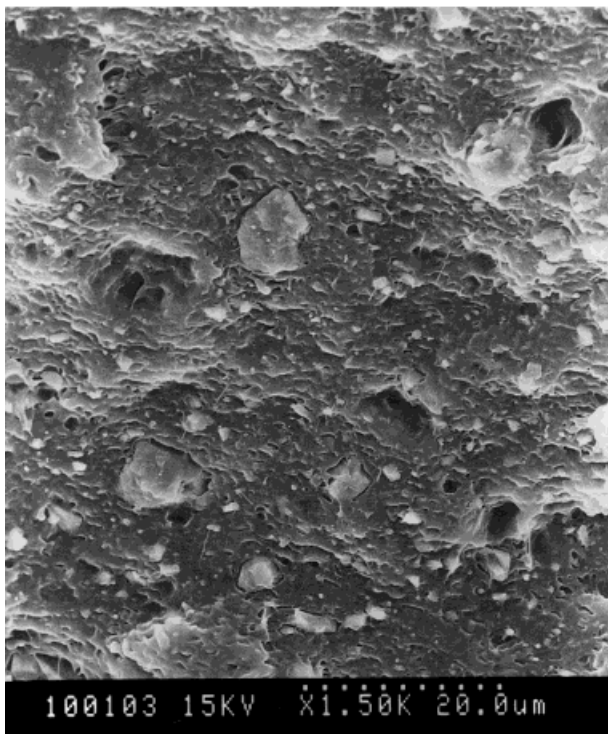
(a)
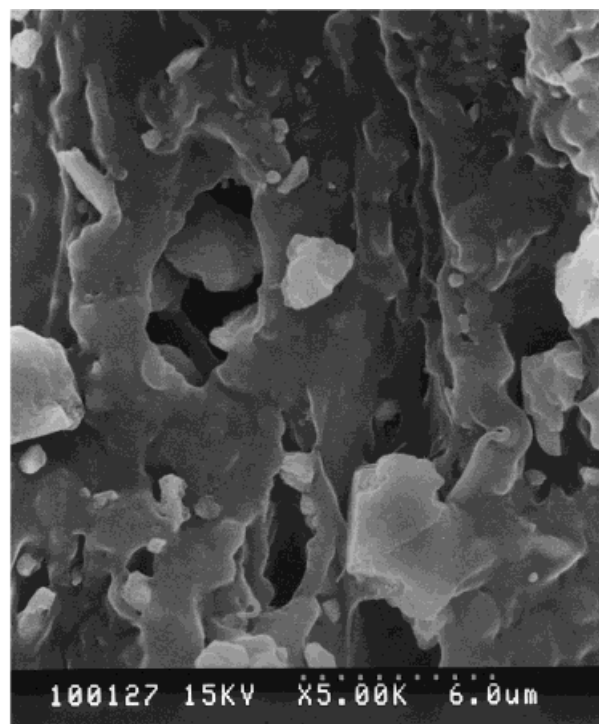
(b)

(c)

Figure 7 Impact fractured surfaces of PP/EOR/CaCO₃. (a) Surface in area (A); (b) surface in area (B); (c) surface in area (C).

(a)

(b)

(c)

Figure 8 Impact fractured surfaces of PP/EVA/CaCO$_3$. (a) Surface in area (A); (b) surface in area (B); (c) surface in area (C).

study by SEM revealed a separation of elastomer and filler particles in the composites containing a nonpolar ethylene–octene copolymer (EOR). An encapsulation of filler by the elastomer was observed in the composites using a polar EVA elastomer. The presence of filler in the EVA phase also was evident from the DSC analysis, in which a decrease in nucleating efficiency of filler on PP was observed in the PP/EVA/CaCO$_3$ systems.

The differences between the mechanical properties of these two types of composites were apparent. Composites with separately dispersed particles of elastomer and filler have lower yield stress, but higher modulus and impact strength than composites with core–shell particles. Analysis of impact fracture morphology revealed that extensive plastic deformation of the PP matrix and cavitation resulted from filler–matrix debonding were important mechanisms in the performance of such composites.

REFERENCES

1. Jancar, J. Macromol. Symp 1996, 108, 163.
2. Hornsby, P. R.; Premphet, K. J Appl Polym Sci 1998, 70, 587.
3. Kolarik, J.; Jancar, J. Polymer 1992, 33, 4961.
4. Pukanszky, B.; Tudos, F.; Kolarik, J.; Lednicky, F. Polym Compos 1990, 11, 98.
5. Kolarik, J.; Pukanszky, B.; Lednicky, F. In Interfaces in Polymer, Ceramic, and Metal Matrix Composites; Ishida, H., Ed.; Science Publishing, 1998, p 453.
6. Kolarik, J.; Lednicky, F.; Jancar, J.; Pukanszky, B. Polym Comm 1990, 31, 201.
7. Jancar, J.; Dibenedetto, A. T. J Mater Sci 1994, 29, 4651.
8. Jancar, J.; Dibenedetto, A. T. J Mater Sci 1995, 30, 1601.
9. Long, Y.; Shanks, R. A. J Appl Polym Sci 1996, 61, 1877.
10. Pukanszky, B.; Kolarik, J.; Lednicky, F. In Polymer Composites; Sedlacek, B., Ed.; Walter de Gruyter, Berlin, 1986, p 553.
11. Kolarik, J.; Lednicky, F. In Polymer Composites; Sedlacek, B., Ed.; Walter de Gruyter, Berlin, 1986, p 537.
12. Kolarik, J.; Pukanszky, B.; Lednicky, F. Comp Polym 1990, 2, 271.
13. Marosi, Gy.; Bertalan, Gy.; Rusznak, I.; Anna, P. Colliod Surfaces 1986, 23, 185.
14. Schaefer, K.; Theinsen, A.; Hess, M.; Kosfeld, R. Polym Eng Sci 1993, 33, 1009.
15. Horanont, P. M.Sc. Thesis, Mahidol University, Thailand, 1999.
16. Kovacevic, V.; Lucic, S.; Cerovecki, Z. Int J Adhesion Adhesives 1997, 17, 239.
17. Premphet, K.; Horanont, P. J Appl Polym Sci 1999, 74, 3445.
18. Nielsen, L. E. J Appl Phys 1970, 41, 4626.
19. Adams, G. C.; Wu, T. K. Failure of Plastics; Hanser Publishers, Munich, 1986, p144.
20. Merle, G.; Yong-Sok, O.; Pillot, C.; Sautereau, H. Polym Testing 1985, 5, 37.
21. Muratoglu, O.K.; Argon, A. S.; Cohen, R. E.; Weinberg, M. Polymer 1995, 36, 921.
22. Bartczak, Z.; Argon, A. S.; Cohen, R. E.; Weinberg, M. Polymer 1999, 40, 2331.